Journal of Water & Health

IWA PUBLISHING

Journal of Water and Health Vol 21 No 3, 372 doi: 10.2166/wh.2023.278

Study on antibacterial properties of heated oyster shell particle against *Bacillus subtilis* spores in rainwater by response surface methodology based on central composite design

Quynh Thi Phuong Tran [a], Balamurugan Ananthakrishnan [b,c] and Hsin-hsin Tung [c,d,*]

[a] Faculty of Environment and Labour Safety, Ton Duc Thang University, Ho Chi Minh City, Viet Nam
[b] FengYu Group, No. 108-2 Minquan Rd., Xindian District, New Taipei City 231, Taiwan
[c] Graduate Institute of Environmental Engineering, National Taiwan University, No. 1, Section 4, Roosevelt Rd., Da'an District, Taipei 10617, Taiwan
[d] Water Innovation, Low Carbon and Environmental Sustainability Research Center, National Taiwan University, Taipei 10617, Taiwan
*Corresponding author. E-mail: htung@ntu.edu.tw

QTPT, 0000-0003-3018-6697; HhT, 0000-0003-2137-2295

ABSTRACT

Taiwan's oyster industry produces shell waste in abundant quantities every year. This study explored the feasibility of applying this resource as a simple and low-cost disinfectant to improve the microbial quality of harvested rainwater. Critical parameters affecting the disinfection efficacy of calcined oyster shell particles, i.e., heating temperature and duration, dosage, and contact time of the calcined shell material against *Bacillus subtilis* endospores in rainwater, were investigated. A central composite design of response surface methodology was employed to study the relative effects. As estimated from R^2 coefficients, a quadratic model was identified to predict the response variable satisfactorily. Results indicated that the heating temperature, dosage, and contact time of the calcined material in the rainwater significantly influenced ($p < 0.05$) the sporicidal effect, consistent with the prior literature on calcined shells of similar nature. However, heating time had a relatively low influence on the sporicidal impact, suggesting that the rate of shell activation, i.e., conversion of the carbonate compound in the shell material to oxide, occurs rapidly at high calcination temperatures. In addition, the sterilization kinetics for heated oyster shell particles in aqueous media under stagnant storage conditions were investigated and found to be in good agreement with Hom's model.

Key words: central composite design, disinfection kinetics, low-cost disinfectant, response surface methodology, waste oyster shell

HIGHLIGHTS

- Sporicidal effects of heated oyster shell on *Bacillus subtilis* endospores were explored.
- Heating temperature, dosage, and contact time of the calcined material have a significant influence on the sporicidal effects.
- Oyster shell heating time has a relatively low influence on the sporicidal effect compared to temperature.
- The heated oyster shell can be potential antibacterial building material for rainwater storage tanks.

1. INTRODUCTION

Oysters, a nutrient-rich bivalve mollusk (Chakraborty *et al.* 2016; Zhu *et al.* 2018; Maurya 2021), can be found in many parts of the world. They inhabit salty or brackish coastal waters, congregating on old shells, rocks, piers, or hard, submerged surfaces. In Taiwan, oyster cultivation accounts for more than one-sixth of the total aquaculture area, generating more than 2 billion USD in annual revenue (Vaschenko *et al.* 2013). Along the western coast of Taiwan, oyster fields stretch from Xiangshan in Hsinchu City in the north to Dapeng Bay in Pingtung County in the south (Liu *et al.* 2015; Ueng *et al.* 2020). Although oyster farming has substantial economic potential, the environmental impact from its by-products/wastes is unavoidable. Oyster shells (OSs) abandoned along the coast can cause a variety of health and environmental issues, involving noxious odors (Chilakala *et al.* 2019; Sadeghi *et al.* 2019) from the decomposition of remaining attached flesh, natural water contamination, soil pH increase, and marine ecosystem modification (Mohamed *et al.* 2012b; Li *et al.* 2015; Thenepalli *et al.* 2017).

According to the Council of Agriculture, an estimated 160,000 metric tons of OSs are generated annually as marine industrial waste in Taiwan, placing a significant burden on the fishing community in waste management and disposal (Hwang &

Weng 2017). Many efforts toward sustainable recycling of OS waste into value-added products have been made (Hellen *et al.* 2019; Jovic *et al.* 2019; Andrade *et al.* 2020; Bonnard *et al.* 2020). With the main components being aragonite and calcite (Chilakala Ramakrishna & Whan 2018) ($CaCO_3 > 95$ wt.%), OSs can be a renewable natural calcium resource for well-known applications, especially as an alkali activator in the production of unfired fly ash bricks (Li *et al.* 2015; Mo *et al.* 2018; Thomas *et al.* 2020) or as filler in composites (Lee *et al.* 2014; AlBadr *et al.* 2020), bio-concrete production (Hong *et al.* 2021), agricultural supplements (Lee *et al.* 2008; Mako *et al.* 2017; Hellen *et al.* 2019), pollutant remediation (Chiou *et al.* 2014; Xu *et al.* 2019; Khirul *et al.* 2020; Xu *et al.* 2021; Zheng *et al.* 2022), soil quality improvement (Ok *et al.* 2011; Torres-Quiroz *et al.* 2021; Wu *et al.* 2022), and high-tech polymer synthesis (Li *et al.* 2017). When calcined at 550 °C and above, the calcite structure of OSs transforms into calcium oxide (CaO) (Kwon *et al.* 2004; Alidoust *et al.* 2015; Huh *et al.* 2016), a promising versatile raw material. OS-derived CaO powder can be utilized in medical preparations to prevent osteoporosis or treat diseases related to calcium metabolism (Bonnard *et al.* 2020), and in industries as a catalyst, material synthesis (Rujitanapanich *et al.* 2014; Khan *et al.* 2018), or a standard reagent (Ferraz *et al.* 2019). Calcined OS is also a potential antibacterial agent with strong antimicrobial properties, diverse bactericidal mechanisms, and biocompatibility (Sadeghi *et al.* 2019).

Taiwan receives more than 2.6 times the global average rainfall (Hsu & Hung 2019). However, water scarcity on the island has reached alarming levels in recent years due to topographical factors and the rapid expansion of industries. Semiconductor manufacturing and agriculture are the two main economic drivers of the island, both heavily dependent on water. On this account, Taiwan has pushed for strategic measures to promote the sustainable development of water resources, which requires initiatives such as rainwater harvesting in urban and rural settlements. A fundamental problem often encountered with this approach is that the water extracted through rainwater harvesting systems is exposed to contaminants from various sources (Schets *et al.* 2010; Hamilton *et al.* 2017).

Harvested rainwater's overall physical, chemical, and microbiological qualities degrade rapidly during storage without proper treatment, resulting in change in odor, color, and taste, making it unsuitable for direct or indirect use. Therefore, it is important to obtain a cost-effective way to inactivate microorganisms in stored rainwater. *Bacillus* produces spores during their stationary phase of development, which are capable of long dormancy and are also highly resistant to heat, radiation, and toxic chemicals (Sunde *et al.* 2009). *Bacillus* spore inactivation can be utilized as a standard for the decontamination of biological agents from drinking water infrastructure due to their disinfection resistance (Szabo *et al.* 2017). A simple yet effective solution being explored is processed seashells, a promising alternative material for low-cost water treatment and disinfection. The antibacterial activity of calcined seashells is related to CaO by two mechanisms in which the primary mechanism is the alkalinity of the medium and the secondary mechanism is the generation of Ca^{2+} and reactive oxygen species (ROS) on the surface of CaO, leading to cell wall rupture. Unlike other shells, OSs are explored less for this application. Therefore, for the practical application of heated oyster shell particles (HOSP) as a disinfectant, it is necessary to understand the effect of different processing and activation parameters contributing to its sterilization potency.

This study investigated the sporicidal activity of HOSP against *Bacillus subtilis* spores. The relative effects of four operating parameters – (i) OS particle heating temperature, (ii) OS particle heating duration, (iii) HOSP concentration, and (iv) treatment time – on disinfection efficacy were assessed by employing response surface methodology (RSM) based on a five-level, four-factorial central composite design (CCD). Besides, a kinetic analysis of the bactericidal action of HOSP was also determined.

2. MATERIALS AND METHODS

2.1. Heated oyster shell particle preparation

Figure 1 depicts the process of calcining oyster shell wastes (*Crassostrea* sp.), locally sourced from Chiayi County, Taiwan, to produce HOSPs. Shells were scrubbed and soaked overnight in tap water to remove salt, biomass, and other surface residues before rinsing in deionized water. Washed shells were dried at 60 °C for 24 h and then ground thoroughly with a commercial grinder and passed through a 150-μm stainless steel sieve (Advantech L3-S100 Standard Sieve, USA series: #100) to collect natural oyster shell particles (OSPs). Fine OSP was calcined in a muffle furnace at the desired temperature (600–1,000 °C) and duration (10–50 min) to obtain HOSP. Their qualitative composition was inspected using a Bruker D8 Advance X-ray diffractometer (XRD) with CuKα radiation at 40 kV and 40 mA, a 2θ range of 15–65° with a step size of 0.05° and a scan speed of 0.25°/min.

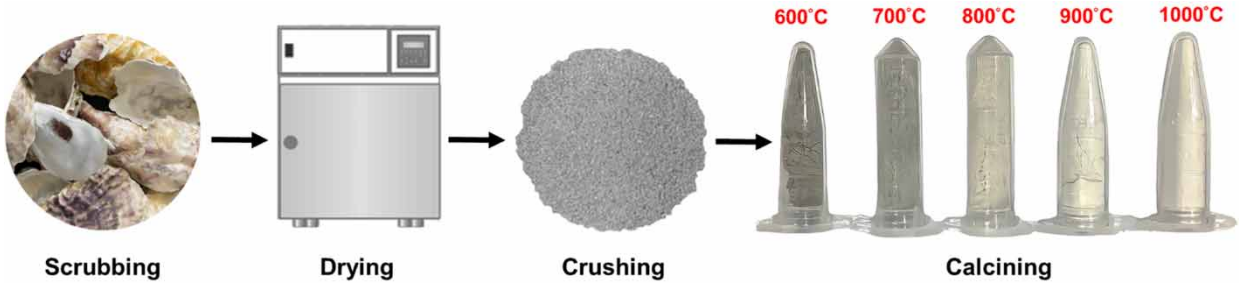

Figure 1 | HOSP production process.

2.2. Nutrient media, microorganisms, and rainwater

Nutrient medium for the growth/cultivation of *B. subtilis* was prepared with 5 g of peptone and 3 g of beef extract for a 1 L solution. The pH of the medium was adjusted to 7.0 with phosphate buffer. For agar medium, bacteriological agar was added at 2% to the aforementioned preparation.

B. subtilis (ATCC 6051) endospores were cultured based on a modified protocol described by Morris (2012). Harvested endospore stock was serially diluted using 0.001 M phosphate-buffered saline solution (PBS) and spread on nutrient agar plates to check their quality and quantity. An average of 9.2×10^8 CFU/mL was observed in the harvested stock.

Fresh rainwater was harvested locally from the rooftop, funneled, and collected directly into sterile glass containers. Harvested rainwater was then pasteurized at 63 °C for 30 min before storing aseptically for further use. The characteristics of pasteurized rainwater are summarized in Table 1.

2.3. HOSP treatment against *B. subtilis* spores

The bactericidal effect of HOSP was examined against *B. subtilis* endospores in a rainwater test medium. All experiments were performed at 25 ± 1 °C under stagnant conditions in a 15 mL sterile centrifuge tube. Powder slurry was prepared by dissolving HOSP into 10 mL of rainwater. Endospore suspension was pipetted to the slurry aseptically at a concentration of 5.7 $\log_{10}$ (colony-forming units per millimeter [CFU/mL]) (i.e., 5×10^5 CFU/mL). Samples were periodically taken, diluted in sterile 0.001 M PBS, and spread thoroughly over agar plates in duplicates. Colonies were counted as CFU/mL after incubation at 37 °C for 72 h. Antibacterial activity was determined by calculating the log inactivation rate of the test organism using Equation (1):

$$\text{Log inactivation} = \log_{10}\frac{N}{N_0} \tag{1}$$

where N_0 and N are the number of viable bacteria before and after treatment, respectively.

To evaluate the influence of process parameters on the antibacterial activity of HOSP, a combination of RSM and CCD developed by Design-Expert® software version 12.0.7.0 (Stat-Ease, Inc., USA) was adopted. A four-factor, five-level CCD with 30 experimental runs consisting of 16 factorial points, 8 axial points, and 6 replicates at the central point (0, 0, 0, 0) was performed. The inactivation rates of *B. subtilis* spores were chosen as the dependent variable, whereas the independent

Table 1 | Physicochemical characteristics of pasteurized rainwater

Parameters	Unit	Results
Electrical conductivity	μS/cm	30.53
pH	–	5.25
Total organic carbon	mg/L	4.81
Turbidity	NTU	3.22
Total dissolved solids	mg/L	16.07

variables were OSP heating temperature (X_1), OSP heating duration (X_2), HOSP concentration (X_3), and treatment time (X_4). Ranges and values of the independent variables in Table 2 were estimated based on the relevant scientific literature and our preliminary studies.

Experimental data were processed with Design-Expert® software trial version 12.0.7.0 and fitted to a second-order polynomial equation (Cho & Zoh 2007; Younis *et al.* 2014; Mohammadi *et al.* 2017):

$$Y = \beta_0 + \sum_{i=1}^{k} \beta_i X_i + \sum_{i=1}^{k} \beta_{ii} X_i^2 + \sum_{i=j}^{k-1} \sum_{i=j+1}^{k} \beta_{ij} X_i X_j \tag{2}$$

where Y represents the response variable (log inactivation); X_i and X_j are the independent coded variables; β_0 is the intercept term; and β_i, β_{ii}, and β_{ij} are coefficients of the linear, quadratic, and interaction effects, respectively.

2.4. Disinfection kinetics

This study identified an appropriate kinetic model for the inactivation rate of *B. subtilis* endospores against HOSP in rainwater. Commonly used deceleration kinetic models, i.e., the modified Chick–Watsons model, Homs model, and Selleck–Collins model, were applied and tested to find a suitable fit.

The Chick–Watson model is the most commonly used in water treatment as a classical kinetic equation. Although the model is widely used to describe the inactivation kinetics of chemicals, it has limitations in practical applications where the sterilization rate does not change with time. In such cases, other models are used to explain deviations from the Chick–Watson first-order kinetics (Azzellino *et al.* 2011; Idris *et al.* 2017).

To explain a decelerating rate of disinfection, the Collins–Selleck model was developed (Crittenden *et al.* 2012). The Hom model, an empirical generalization of the Chick–Watson pseudo-first-order rate law, is used to address a curvilinear rate of disinfection (Lambert & Johnston 2000). This model – a linear regression of the concentration of the disinfectant, time of treatment, and the survival – is used to examine disinfection data of different organisms and to explain the effect of disinfection systems. HOSP dosage and treatment time were taken as the predictors, and the log of survival ratio of the indicator organisms was taken as the dependent variable. The experimental data were fit to disinfection models shown below.

$$\text{Modified Chick–Watsons: } \ln \frac{N}{N_0} = k_1[1 - \exp(-k_2 t)] \tag{3}$$

$$\text{Collins–Selleck: } \ln \frac{N}{N_0} = -k_{cs}[\ln(Ct) - \ln(b)] \tag{4}$$

$$\text{Hom: } \ln \frac{N}{N_0} = -k_h C^n t^m \tag{5}$$

where N is the number of viable organisms present at time t; N_0 is the number of viable organisms at time 0; k_1 and k_2 are coefficients of specific lethality; k_{cs} is a log-based coefficient of specific lethality; k_h is the inactivation rate constant; b is the lag coefficient; n and m are Hom dilution coefficient and time exponent, respectively; and C is biocide concentration, specifically HOSP concentration.

Table 2 | Independent variables and levels used in CCD for the sporicidal activity against *B. subtilis* spores by HOSP

	Factor levels				
Factors, X_i	**−2**	**−1**	**0**	**+1**	**+2**
OSP heating temperature (°C), X_1	600	700	800	900	1,000
OSP heating duration (min), X_2	10	20	30	40	50
HOSP concentration (mg/mL), X_3	0.1	0.5	0.9	1.3	1.7
Treatment time (h), X_4	0	72	144	216	288

The model that yields the highest coefficient of determination (adjusted R^2) was the best fit for the purpose. To determine the inactivation kinetics and estimate the model parameter, nonlinear multivariate regression analysis was performed using R software for Macintosh, version 3.5.3.

3. RESULTS AND DISCUSSION

3.1. Modeling the bactericidal activity of HOSP

The antibacterial effect of HOSP against *B. subtilis* endospores, expressed as log inactivation, was investigated under various conditions in accordance with the experimental runs indicated by Design-Expert® software version 12.0.7.0. Table 3 summarizes the results of all 30 runs in the CCD matrix for response surface modeling. The observed inactivation rates for *B. subtilis* endospores ranged from −0.02 to 4.86 log. The model predictions were consistent with observed log inactivation.

In CCD studies, model adequacy check is an integral part to guarantee that it gives an adequate estimation for real analysis systems (Arslan-Alaton *et al.* 2009; Ivanescu *et al.* 2016; Arslan & Kara 2017). Approximating model functions would yield inaccurate or misleading results if the fit were poor (Körbahti 2007; Arslan & Kara 2017). The quality of the proposed model was evaluated by constructing a diagnostic plot between the predicted and actual log inactivation values. As shown in Supplementary Material, Figure S1(a), no significant difference was found since the data points were very close to the diagonal line. In other words, the predicted values from the developed model agreed well with the observed values in the experimental data. The plot of residuals versus predicted responses is indicated in Supplementary Material, Figure S1(b). The distributions of residuals were random without any trends. Furthermore, a one-way analysis of variance (ANOVA) was tested to check the adequacy of the suggested model, and the results are described in Table 4. The model's *F*-value of 31.62 reveals that the model is statistically fit. A *p*-value less than 0.05 means that the model parameters are highly significant, whereas values greater than 0.1 indicate insignificant terms. In this case, X_1, X_2, X_3, X_4, X_1X_4 (interaction between X_1 and X_4), X_1^2 (second-order effect of X_1), X_3^2 (second-order effect of X_3), and X_4^2 (second-order effect of X_4) are important model terms, and X_2^2 (second-order effect of X_2) is negligible. The large R^2 of 0.9343 shows a high degree of consistency between the observed and calculated results. The quality of fit estimates from the coefficients R^2 represents a reasonable agreement between the predicted R^2 and the adjusted R^2 (the difference is less than 0.2), implying that the model provides an adequate fit for the data. A signal-to-noise ratio of 20.7114 provides an adequate signal, demonstrating that the chosen model can be used to navigate the design space. Consequently, the proposed reduced quadratic model represents the best approach for the relationship between variables and responses and is sufficient to assess the effects of variables.

Once high dependability was established, predictions about the antibacterial efficacy of HOSP disinfectant could be obtained through the reduced second-order polynomial equations with coded and actual variables as Equations (6) and (7), respectively.

Final equation in terms of coded factors:

$$Y = 3.31 + 0.6125X_1 + 0.2283X_2 + 0.8508X_3 + 0.9433X_4 + 0.23X_1X_4 - 0.3333X_1^2 - 0.1346X_2^2 - 0.2133X_3^2 - 0.3033X_4^2 \quad (6)$$

where Y is the log inactivation response for *B. subtilis* endospores; X_1, X_2, X_3, and X_4 are OSP heating temperature, OSP heating duration, HOSP concentration, and treatment time, respectively.

Final equation in terms of actual factors are as follows:

$$\begin{aligned}\log \text{inactivation} = {} & -27.23063 + 0.054858 \times (\text{OSP heating temp}) \\ & + 0.103583 \times (\text{OSP heating duration}) + 4.52708 \times [\text{HOSP}] \\ & + 0.004398 \times (\text{treatment time}) \\ & + 0.000032 \times (\text{OSP heating temp}) \times (\text{treatment time}) \\ & - 0.000033 \times (\text{OSP heating temp})^2 - 0.001346 \times (\text{OSP heating duration})^2 \\ & - 1.33333 \times ([\text{HOSP}])^2 - 0.000059 \times (\text{treatment time})^2\end{aligned} \quad (7)$$

Table 3 | Five-level/four-factor CCD matrix along with log inactivation response for *B. subtilis* endospores

	Coded values				Real values				Log inactivation ($\log_{10}(N/N_0)$)	
Run order	X_1	X_2	X_3	X_4	OSP heating temperature (°C)	OSP heating duration (min)	HOSP conc. (mg/mL)	Treatment time (h)	Observed	Predicted
1	−2	0	0	0	600	30	0.9	144	0.66	0.76
2	−1	−1	−1	+1	700	20	0.5	216	0.49	1.35
3	−1	+1	+1	+1	700	40	1.3	216	3.75	3.51
4	−1	−1	−1	−1	700	20	0.5	72	0.18	−0.08
5	−1	+1	−1	+1	700	40	0.5	216	1.83	1.81
6	−1	+1	+1	−1	700	40	1.3	72	2.36	2.08
7	−1	−1	+1	−1	700	20	1.3	72	1.07	1.63
8	−1	+1	−1	−1	700	40	0.5	72	0.73	0.38
9	−1	−1	+1	+1	700	20	1.3	216	3.37	3.05
10	0	0	0	0	800	30	0.9	144	3.57	3.31
11	0	−2	0	0	800	10	0.9	144	2.73	2.32
12	0	0	0	0	800	30	0.9	144	3.57	3.31
13	0	0	0	−2	800	30	0.9	0	−0.02	0.21
14	0	+2	0	0	800	50	0.9	144	2.96	3.23
15	0	0	−2	0	800	30	0.1	144	1.05	0.76
16	0	0	+2	0	800	30	1.7	144	4.01	4.16
17	0	0	0	0	800	30	0.9	144	3.57	3.31
18	0	0	0	+2	800	30	0.9	288	4.36	3.99
19	0	0	0	0	800	30	0.9	144	3.12	3.31
20	0	0	0	0	800	30	0.9	144	3.25	3.31
21	0	0	0	0	800	30	0.9	144	2.80	3.31
22	+1	+1	+1	+1	900	40	1.3	216	4.43	5.19
23	+1	−1	+1	−1	900	20	1.3	72	2.77	2.39
24	+1	+1	+1	−1	900	40	1.3	72	2.99	2.85
25	+1	−1	+1	+1	900	20	1.3	216	4.86	4.74
26	+1	−1	−1	−1	900	20	0.5	72	0.49	0.69
27	+1	+1	−1	+1	900	40	0.5	216	3.95	3.49
28	+1	−1	−1	+1	900	20	0.5	216	2.61	3.04
29	+1	+1	−1	−1	900	40	0.5	72	0.82	1.15
30	+2	0	0	0	1000	30	0.9	144	3.44	3.21

The regression model provides the preferred effects of the selected variables as X_4 (treatment time) $> X_3$ (HOSP concentration) $> X_1$ (OSP heating temperature) $> X_2$ (OSP heating duration).

3.2. Effects of selected variables on the bactericidal activity of HOSP

Three-dimensional surface plots and two-dimensional contours of the responses – where one variable was fixed at the center point, and the others varied over the experimental ranges – were applied to determine the relative effects of selected variables on the bactericidal activity of HOSP. OS particle heating temperature and duration, HOSP concentration, and treatment time could all have a positive or negative effect on *B. subtilis* endospores removal rate, as shown in Figures 2 and 3. Peak performance with 5.58 log inactivation was predicted at $T_{\text{heating OSP}} = 926$ °C, $t_{\text{heating OSP}} = 34$ min, [HOSP] = 1.39 mg/mL, and $t_{\text{treatment}} = 271$ h.

Table 4 | ANOVA for the reduced quadratic model

Source	Sum of squares	df	Mean square	*F*-value	*p*-value	Remark
Model	55.27	9	6.14	31.62	<0.0001	***
X_1	9.00	1	9.00	46.36	<0.0001	***
X_2	1.25	1	1.25	6.44	0.0196	***
X_3	17.37	1	17.37	89.45	<0.0001	***
X_4	21.36	1	21.36	109.96	<0.0001	***
X_1X_4	0.8464	1	0.8464	4.36	0.0498	***
X_1^2	3.05	1	3.05	15.69	0.0008	***
X_2^2	0.4968	1	0.4968	2.56	0.1254	*
X_3^2	1.25	1	1.25	6.43	0.0197	***
X_4^2	2.52	1	2.52	12.99	0.0018	***
Residual	3.88	20	0.1942			
Lack of fit	3.38	15	0.2255	2.24	0.1902	*
Pure error	0.5025	5	0.1005			
Cor total	59.15	29				
Fit statistics						
Standard deviation		0.4407		R^2	0.9343	
Coefficient of variation (%)		17.45		Adjusted R^2	0.9048	
Adeq precision		20.7114		Predicted R^2	0.8403	

Note: *Not significant ($p \geq 0.1$).
**Significant ($0.05 \leq p < 0.1$).
***Highly significant ($p < 0.05$).

The interactive effects of oyster shell particle heating temperature (X_1) and duration (X_2) on the inactivation rate of *B. subtilis* endospores are shown in Figure 2. The HOSP concentration (X_3) and treatment time (X_4) were unchanged at 0.9 mg/mL and 144 h, respectively, while other variables were varied in the ranges of 600–1,000 °C with X_1 and 10–50 min with X_2. As seen in the plots, increasing the calcining temperature positively affected the inactivation rate at all tested conditions. Sterilization efficiency rapidly increased from 0.755 $\log_{10}$ to 3.205 $\log_{10}$ with an increase in OSP calcining temperature from 600 to 1,000 °C, at 30 min heating duration. Meanwhile, the observed change was relatively low with heating duration across all tested heating temperatures. The results correlate well with the previous reports of heat-activated conditions for materials derived from scallop (Sawai 2011) and blood cockle shells (Mohamed *et al.* 2012a, 2012b). Increasing the temperature during calcination leads to increased conversion of calcium carbonate ($CaCO_3$) to calcium oxide (CaO), Equation (8), producing more CaO per mass of the calcined shell. X-ray diffraction analyses (Supplementary Material, Figure S2) have shown that $CaCO_3$ decomposition in OSs occurs above 600 °C, with XRD peaks for CaO detected above 800 °C – where decomposition mass mainly consists of a mixture of calcium carbonate and crystalline calcium oxide – leading to a complete conversion at 900 °C where all the calcium in the heated mass exists as calcium oxide.

$$CaCO_3 \xrightarrow{\Delta} CaO + CO_2 \uparrow \tag{8}$$

In aqueous media, both alkalinity and ROS generated from CaO hydration (Equation (9)) have been determined for their bactericidal effects on a wide range of bacterial and fungal organisms (Sawai 2011; Yasue *et al.* 2011, 2014; Watanabe *et al.* 2014; Hijikata *et al.* 2016; Liang *et al.* 2022). The antimicrobial effect of hydroxyl ions is understood to be protein denaturation and damage to bacterial cytoplasmic membranes and DNA (Mohammadi *et al.* 2012). A similar effect was observed on MS2 coliphage viral bodies, where capsid damage and partial RNA exteriorization are seen to accompany a pH increase. Meanwhile, alkaline inactivation of *Escherichia coli* is understood as a process that damages the outer membrane and their enzymatic activities, thereby damaging nucleic acids and/or metabolism (Hijikata *et al.* 2016). Further studies into

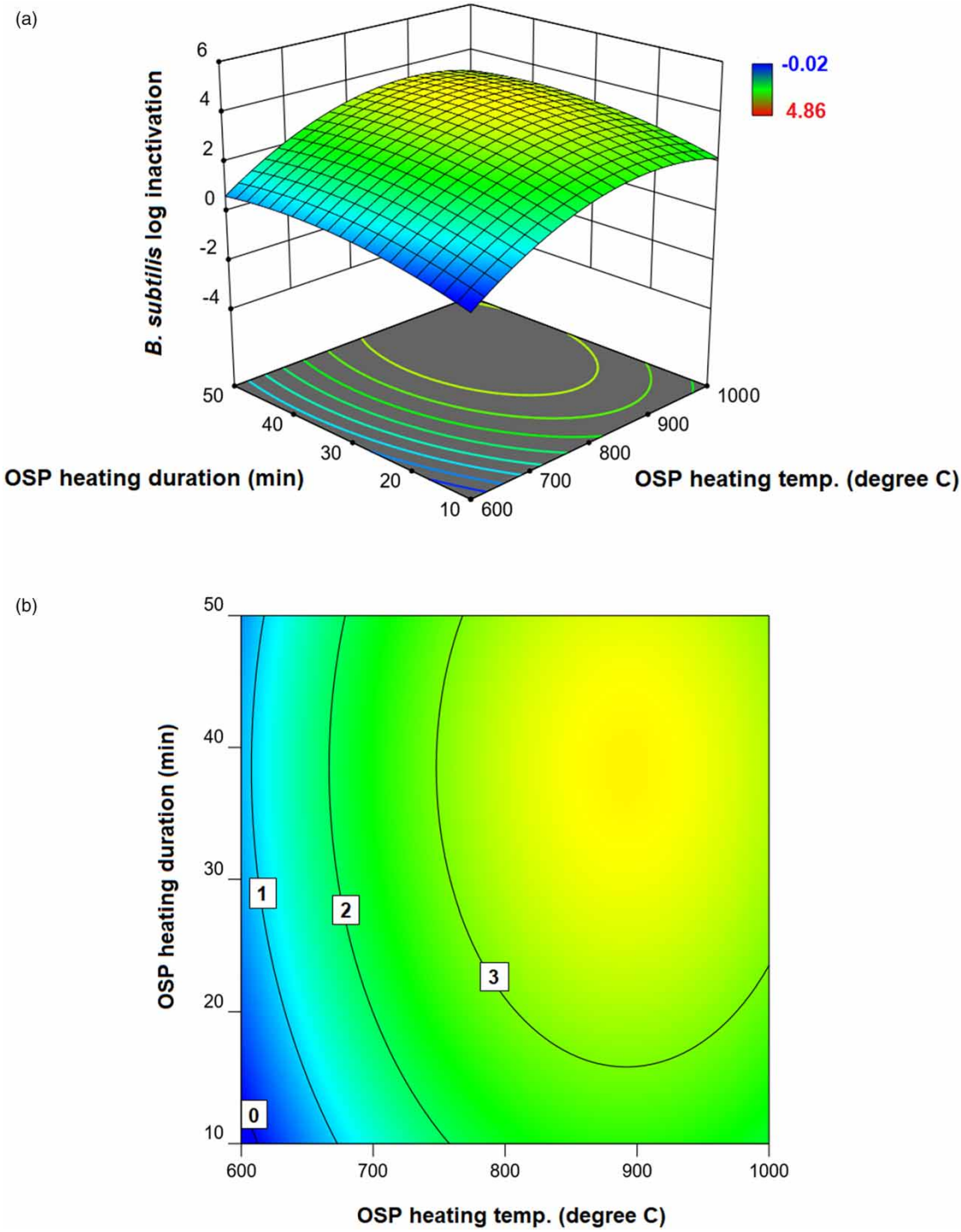

Figure 2 | 3D response surface (a) and contour (b) plots for *B. subtilis* inactivation as a function of oyster shell particle heating temperature and duration. HOSP concentration and treatment time were kept constant at 0.9 mg/mL and 144 h, respectively. *B. subtilis* log inactivation ranges from −0.02 to 4.86, where warmer (colder) colors indicate higher (lower) values. Please refer to the online version of this paper to see this figure in colour: http://dx.doi.org/10.2166/wh.2023.278.

CaO-based disinfectants derived from heated surf clam, scallop shell, dolomite (a double salt composed of $CaCO_3$ and $MgCO_3$), and ceramic (a composite of oxides of calcium (CaO), magnesium (MgO), and zinc (ZnO)) have also strongly suggested the involvement of ROS in the microbicidal effect. Yasue *et al.* (2011) have shown that the sporicidal effect of

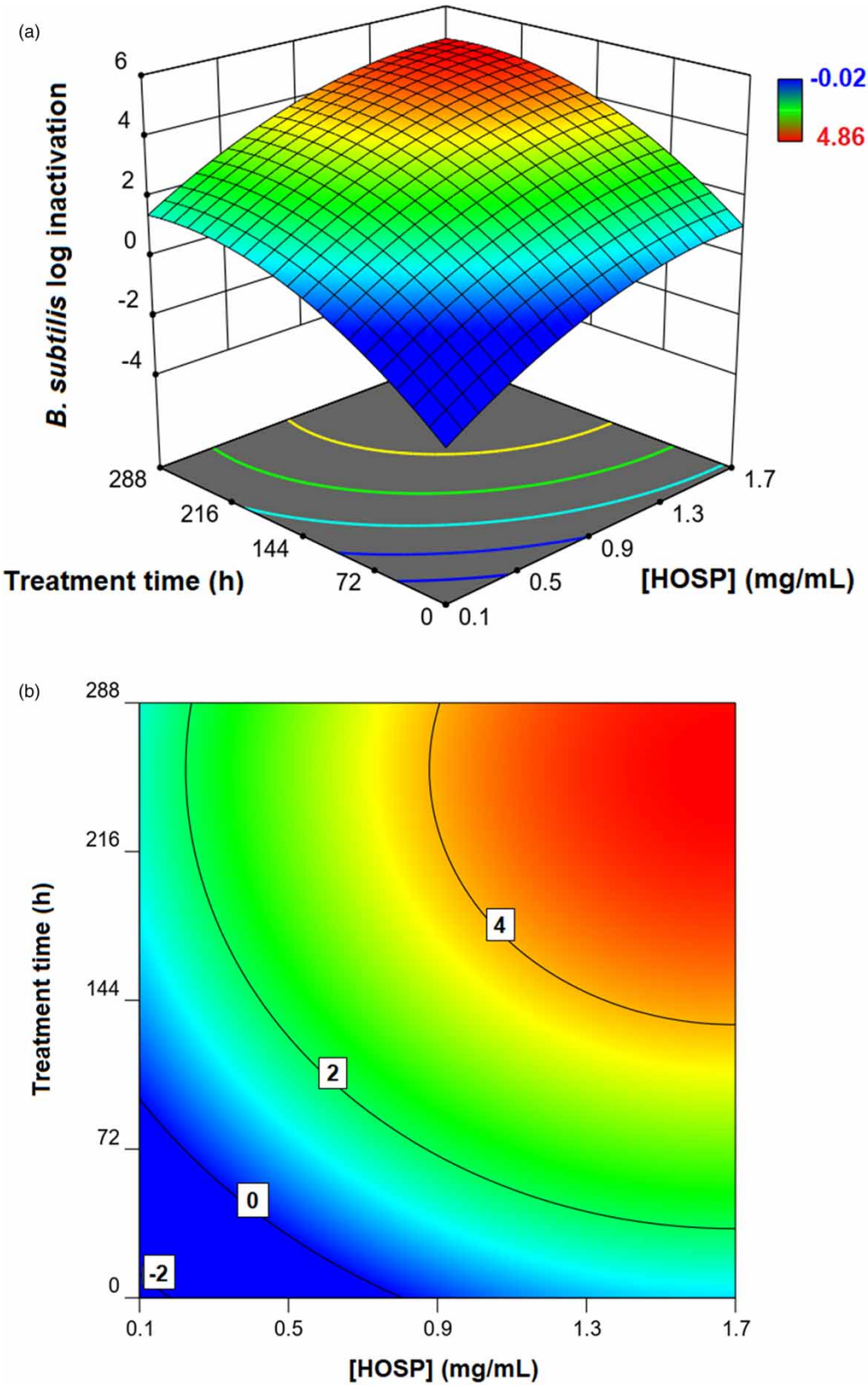

Figure 3 | 3D response surface (a) and contour (b) plots for *B. subtilis* inactivation as a function of HOSP concentration and treatment time. OSP heating temperature and duration were kept constant at 800 °C and 30 min, respectively.

heated dolomite powder slurry at pH 12.7 was much higher than that of NaOH at pH 13. Chemiluminescence analysis indicated that active oxygen species generated from the slurry was one of the critical factors associated with the sporicidal activity. A similar conclusion was reached in other related studies involving heated scallop shells and ceramic powder (Bae *et al.* 2006; Sawai 2011; Watanabe *et al.* 2014). Results predicted in the current study suggest that calcined OSPs are generally identical in characteristics and properties as a potential source for natural disinfectants as calcined scallops, cockle, or clam shells.

$$CaO(s) + H_2O(l) \rightarrow Ca^{2+}(aq) + 2OH^{-}(aq) \tag{9}$$

Figure 2 shows the effect of HOSP dosage and treatment time on the inactivation rate at constant shell heating time and temperature of 30 min and 800 °C, respectively. The inactivation rate was predicted to increase steadily with both parameters. Specifically, the bactericidal effects of HOSP rapidly increased from 0.677 $\log_{10}$ to 4.080 $\log_{10}$ with an increase in HOSP dosage from 0.1 to 1.7 mg/mL at 144 h treatment time. The more HOSPs used, the more CaO is generated, resulting in more ROS generation. This assists in a higher inactivation rate of *B. subtilis* endospores. A similar trend was also observed with the increasing treatment time in the system from 0 to 288 h. The inactivation rate increased from 0.132 $\log_{10}$ to 3.905 $\log_{10}$ at a HOSP concentration of 0.9 mg/mL.

3.3. Kinetic analysis of bactericidal activity against *B. subtilis*

In rainwater medium, the coefficient of determination calculated for the chosen models are presented in Table 5. Here, Hom's empirical model is defined to better describe the experimental data based on R^2 best fit.

Model parameters k, n, and m for Hom's model determined using multiple linear regression is summarized in Table 6. Both parameters are observed to be statistically very significant with $p < 0.05$ at 1×10^{-11} and 2×10^{-16}. Multiple R^2 and adjusted R^2 were reasonably high at 0.9408 and 0.9400, respectively. Hence, the disinfection kinetic for HOSP against *B. subtilis* spores in rainwater medium is defined by Equation (10).

$$\ln \frac{N}{N_0} = -0.0017 \times C^{0.6999} \times t^{1.6887} \tag{10}$$

4. CONCLUSION

The relative effects between OS heat activation and treatment conditions on the sporicidal efficacy were determined using a central composited design of the response surface model. The model indicated that the predicted and experimental values

Table 5 | Coefficient determination for tested kinetic models for *B. subtilis* inactivation in rainwater by OSP heated at 1,000 °C for 10 min

Disinfection kinetic model	R^2	Adjusted R^2
Modified Chick–Watson	0.2551	0.2500
Collin–Selleck	0.6222	0.6196
Hom	0.9408	0.9400

Table 6 | Summary of statistics and regression estimates for the best fit Hom's model for *B. subtilis* inactivation in rainwater

	k	n	m
Estimates	0.0017	0.6999	1.6887
Standard error	0.1725	0.0948	0.0352
Significance ($p < 0.05$)	2×10^{-16}	10^{-11}	2×10^{-16}
N	148		
R^2	0.9408		

were not significantly different. The ANOVA showed that the effects of OS heating temperature, HOSP dosage in the treatment medium, and the treatment time contributed significantly to the sporicidal effects ($p < 0.05$). Polynomial models fitting the predicted response, i.e., log inactivation of the test organism (*B. subtilis*), suggested that the yield of active compound (CaO) in calcined OSs and the resulting microbicidal effect increased with the increase in OS heating temperature and HOSP concentration and contact time in rainwater medium. OS heating duration did not significantly increase the active component yield at a given heating temperature. In addition, the inactivation kinetics for HOSP in aqueous media under stagnant storage conditions are in good agreement with Hom's model. The results from this study may be applied to rainwater harvesting tank construction. Incorporating HOSP in rainwater harvesting tank materials, such as submerged bricks or tank inner lining, may prevent water from fouling during long-term storage. Despite their simplicity and low cost, CaO-based disinfectants have some limitations due to alkaline pH and Ca^{2+} residues in treated rainwater, which presents a major challenge.

ACKNOWLEDGEMENTS

This study was supported by the National Science and Technology, Taiwan (Project 109-2221-E-002-079-MY3) and National Taiwan University Core Consortiums (NTUCCP-111L895102 and 112L893902) within the framework of the Higher Education SPROUT Project by the Ministry of Education (MOE) in Taiwan.

DATA AVAILABILITY STATEMENT

All relevant data are included in the paper or its Supplementary Information.

CONFLICT OF INTEREST

The authors declare there is no conflict.

REFERENCES

AlBadr, R. M., Halfi, S. A. & Ziadan, K. M. 2020 The effectiveness of oyster filler on the physical and mechanical properties of novel dental restorative composite. *AIP Conference Proceedings* **2290** (1), 050001.

Alidoust, D., Kawahigashi, M., Yoshizawa, S., Sumida, H. & Watanabe, M. 2015 Mechanism of cadmium biosorption from aqueous solutions using calcined oyster shells. *Journal of Environmental Management* **150**, 103–110.

Andrade, L. R. S., Cruz, I. A., de Melo, L., Vilar, D. d. S., Fuess, L. T., Reis e Silva, G., Silva Manhães, V. M., Torres, N. H., Soriano, R. N., Bharagava, R. N., Romanholo Ferreira, L. F. & Figueiredo, R. T. 2020 Oyster shell-based alkalinization and photocatalytic removal of cyanide as low-cost stabilization approaches for enhanced biogas production from cassava starch wastewater. *Process Safety and Environmental Protection* **139**, 47–59.

Arslan, F. N. & Kara, H. 2017 Central composite design and response surface methodology for the optimization of Ag^{+}-HPLC/ELSD method for triglyceride profiling. *Journal of Food Measurement and Characterization* **11** (2), 902–912.

Arslan-Alaton, I., Tureli, G. & Olmez-Hanci, T. 2009 Treatment of azo dye production wastewaters using photo-Fenton-like advanced oxidation processes: optimization by response surface methodology. *Journal of Photochemistry and Photobiology A: Chemistry* **202** (2), 142–153.

Azzellino, A., Antonelli, M., Canziani, R., Malpei, F., Marinetti, M. & Nurizzo, C. 2011 Multivariate modelling of disinfection kinetics: a comparison among three different disinfectants. *Desalination and Water Treatment* **29** (1–3), 128–139.

Bae, D. H., Yeon, J. H., Park, S. Y., Lee, D. H. & Ha, S. D. 2006 Bactericidal effects of CaO (scallop-shell powder) on foodborne pathogenic bacteria. *Archives of Pharmcal Research* **29** (4), 298–301.

Bonnard, M., Boury, B. & Parrot, I. 2020 Key insights, tools, and future prospects on oyster shell end-of-life: a critical analysis of sustainable solutions. *Environmental Science & Technology* **54**, 26–38.

Chakraborty, K., Chakkalakal, S. J., Joseph, D. & Joy, M. 2016 Nutritional composition of edible oysters (*Crassostrea madrasensis L.*) from the southwest coast of India. *Journal of Aquatic Food Product Technology* **25** (8), 1172–1189.

Chilakala Ramakrishna, T. T. & Whan, A. J. 2018 A brief review on oyster shells origin and sedimentary evolution for the formation of limestone. *Journal of Energy Engineering* **27** (3), 48–56.

Chilakala, R., Thannaree, C., Shin, E. J., Thenepalli, T. & Ahn, J. W. 2019 Sustainable solutions for oyster shell waste recycling in Thailand and the Philippines. *Recycling* **4** (3), 35–44.

Chiou, I. J., Chen, C. H. & Li, Y. H. 2014 Using oyster-shell foamed bricks to neutralize the acidity of recycled rainwater. *Construction and Building Materials* **64**, 480–487.

Cho, I.-H. & Zoh, K.-D. 2007 Photocatalytic degradation of azo dye (Reactive Red 120) in TiO_2/UV system: optimization and modeling using a response surface methodology (RSM) based on the central composite design. *Dyes and Pigments* **75** (3), 533–543.

Crittenden, J. C., Rhodes Trussell, R., Hand, D. W., Howe, K. J. & Tchobanoglous, G. 2012 *MWH's Water Treatment: Principles and Design*, 3rd edn. John Wiley & Sons, Hoboken, NJ.

Ferraz, E., Gamelas, J. A. F., Coroado, J., Monteiro, C. & Rocha, F. 2019 Recycling waste seashells to produce calcitic lime: characterization and wet slaking reactivity. *Waste and Biomass Valorization* **10** (8), 2397–2414.

Hamilton, K. A., Ahmed, W., Palmer, A., Smith, K., Toze, S. & Haas, C. N. 2017 Seasonal assessment of opportunistic premise plumbing pathogens in roof-harvested rainwater tanks. *Environmental Science & Technology* **51** (3), 1742–1753.

Hellen, T., Mesquita-Guimarães, J., Henriques, B., Silva, F. & Fredel, M. 2019 The potential use of oyster shell waste in new value-added by-product. *Resources* **8**, 1–15.

Hijikata, N., Tezuka, R., Kazama, S., Otaki, M., Ushijima, K., Ito, R., Okabe, S., Sano, D. & Funamizu, N. 2016 Bactericidal and virucidal mechanisms in the alkaline disinfection of compost using calcium lime and ash. *Journal of Environmental Management* **181**, 721–727.

Hong, M., Jang, I., Son, Y., Yi, C. & Park, W. 2021 Agricultural by-products and oyster shell as alternative nutrient sources for microbial sealing of early age cracks in mortar. *AMB Express* **11** (1), 1–15.

Hsu, C.-H. & Hung, C.-Y. 2019 Sustainable development of climate change resources: about recycling of water resources in Maple Park, Taichung, Taiwan. *E3S Web of Conferences* **117**, 00016.

Huh, J.-H., Choi, Y.-H., Lee, H.-J., Choi, W., Chilakala, R., Lee, H.-W., Lee, S.-H. & Ahn, J.-W. 2016 The use of oyster shell powders for water quality improvement of Lakes by algal blooms removal. *Journal of the Korean Ceramic Society* **53**, 1–6.

Hwang, C. C. & Weng, C. H. 2017 Key factors contributing to simultaneous nitrification-denitrification in a biological aerated filter system using oyster shell medium. *Environment Protection Engineering* **43**, 75–86.

Idris, M., Hammed, A., Jami, M. & Jamal, P. 2017 Multivariate regression analysis of disinfection kinetics using *Moringa oleifera* defatted seed extract. *ARPN Journal of Engineering and Applied Sciences* **12** (7), 2248–2253.

Ivanescu, A. E., Li, P., George, B., Brown, A. W., Keith, S. W., Raju, D. & Allison, D. B. 2016 The importance of prediction model validation and assessment in obesity and nutrition research. *International Journal of Obesity (London)* **40** (6), 887–894.

Jovic, M., Mandic, M., Sljivic-Ivanovic, M. & Smičiklas, I. 2019 Recent trends in application of shell waste from mariculture. *Studia Marina* **32**, 47–62.

Khan, M. D., Ahn, J. W. & Nam, G. 2018 Environmental benign synthesis, characterization and mechanism studies of green calcium hydroxide nano-plates derived from waste oyster shells. *Journal of Environmental Management* **223**, 947–951.

Khirul, M. A., Kim, B.-G., Cho, D., Yoo, G. & Kwon, S.-H. 2020 Effect of oyster shell powder on nitrogen releases from contaminated marine sediment. *Environmental Engineering Research* **25** (2), 230–237.

Körbahti, B. K. 2007 Response surface optimization of electrochemical treatment of textile dye wastewater. *Journal of Hazardous Materials* **145** (1), 277–286.

Kwon, H.-B., Lee, C.-W., Jun, B.-S., Yun, J.-d., Weon, S.-Y. & Koopman, B. 2004 Recycling waste oyster shells for eutrophication control. *Resources, Conservation and Recycling* **41** (1), 75–82.

Lambert, R. J. & Johnston, M. D. 2000 Disinfection kinetics: a new hypothesis and model for the tailing of log-survivor/time curves. *Journal of Applied Microbiology* **88** (5), 907–913.

Lee, C., Lee, D., Ali, M. & Kim, P. 2008 Effects of oyster shell on soil chemical and biological properties and cabbage productivity as a liming material. *Waste Management (New York, N.Y.)* **28**, 2702–2708.

Lee, D.-W., Kim, B.-S. & Song, J.-I. 2014 Development and characterization of oyster shell powder filled polypropylene composite. *Composites Research* **27** (5), 201–206.

Li, G., Xu, X., Chen, E., Fan, J. & Xiong, G. 2015 Properties of cement-based bricks with oyster-shells ash. *Journal of Cleaner Production* **91**, 279–287.

Li, L., Zeng, Z., Wang, Z., Peng, Z., She, X., Li, S. & Zhong, J. 2017 Effect of oyster shell powder loading on the mechanical and thermal properties of natural rubber/oyster shell composites. *Polymers and Polymer Composites* **25** (1), 17–22.

Liang, X., Dai, R., Chang, S., Wei, Y. & Zhang, B. 2022 Antibacterial mechanism of biogenic calcium oxide and antibacterial activity of calcium oxide/polypropylene composites. *Colloids and Surfaces A: Physicochemical and Engineering Aspects* **650**, 129446.

Liu, T.-K., Kao, J.-C. & Chen, P. 2015 Tragedy of the unwanted commons: governing the marine debris in Taiwan's oyster farming. *Marine Policy* **53**, 123–130.

Mako, A., Jemiseye, B., Abokede, F. & Adedeji, B. 2017 Comparative use of oyster shell and limestone as sources of calcium in the diet of laying chickens. *Nigerian Journal of Animal Production* **44**, 275–281.

Maurya, N. K. 2021 Nutraceutical potential of Oyster. *Research & Reviews Journal of Food Science and Technology* **10** (1), 1–6.

Mo, K. H., Alengaram, U. J., Jumaat, M. Z., Lee, S. C., Goh, W. I. & Yuen, C. W. 2018 Recycling of seashell waste in concrete: a review. *Construction and Building Materials* **162**, 751–764.

Mohamed, M., Rashidi, N. A., Yusup, S., Teong, L. K., Rashid, U. & Ali, R. M. 2012a Effects of experimental variables on conversion of cockle shell to calcium oxide using thermal gravimetric analysis. *Journal of Cleaner Production* **37**, 394–397.

Mohamed, M., Yousuf, S. & Maitra, S. 2012b Decomposition study of calcium carbonate in cockle shell. *Journal of Engineering Science and Technology* **7**, 1–10.

Mohammadi, Z., Shalavi, S. & Yazdizadeh, M. 2012 Antimicrobial activity of calcium hydroxide in endodontics: a review. *Chonnam Medical Journal* **48**, 133–140.

Mohammadi, L., Bazrafshan, E., Noroozifar, M., Moghaddama, A. R., Feizabad, A. R. & Mahvi, A. 2017 Optimization of the catalytic ozonation process using copper oxide nanoparticles for the removal of benzene from aqueous solutions. *Global Journal of Environmental Science and Management* **3**, 403–416.

Morris, J. P. 2012 *Disinfection of Bacillus subtilis Spores Using Ultraviolet Light Emitting Diodes*. Doctoral Dissertation, Ohio University, OH.

Ok, Y. S., Lim, J. E. & Moon, D. H. 2011 Stabilization of Pb and Cd contaminated soils and soil quality improvements using waste oyster shells. *Environmental Geochemistry and Health* **33** (1), 83–91.

Rujitanapanich, S., Kumpapan, P. & Wanjanoi, P. 2014 Synthesis of hydroxyapatite from oyster shell via precipitation. *Energy Procedia* **56**, 112–117.

Sadeghi, K., Park, K. & Seo, J. 2019 Oyster shell disposal: potential as a novel ecofriendly antimicrobial agent for packaging : a mini review. *Korean Journal of Packaging Science and Technology* **25**, 57–62.

Sawai, J. 2011 Antimicrobial characteristics of heated scallop shell powder and its application. *Biocontrol Science* **16** (3), 95–102.

Schets, F. M., Italiaander, R., van den Berg, H. H. & de Roda Husman, A. M. 2010 Rainwater harvesting: quality assessment and utilization in The Netherlands. *Journal of Water and Health* **8** (2), 224–235.

Sunde, E. P., Setlow, P., Hederstedt, L. & Halle, B. 2009 The physical state of water in bacterial spores. *Proceedings of the National Academy of Sciences* **106** (46), 19334–19339.

Szabo, J. G., Meiners, G., Heckman, L., Rice, E. W. & Hall, J. 2017 Decontamination of *Bacillus* spores adhered to iron and cement-mortar drinking water infrastructure in a model system using disinfectants. *Journal of Environmental Management* **187**, 1–7.

Thenepalli, T., Chilakala, R. & Ahn, J.-W. 2017 Environmental effect of the coffee waste and anti-microbial property of oyster shell waste treatment. *Journal of Energy Engineering* **26**, 39–49.

Thomas, J. I., Jose, J., Mathew, N. R., Reji, R., 2020 Mud Bricks Using Oyster Shells. In: *Proceedings of SECON'19: Structural Engineering and Construction Management 3*. Springer International Publishing, Cham, pp. 205–211.

Torres-Quiroz, C., Dissanayake, J. & Park, J. 2021 Oyster shell powder, zeolite and red mud as binders for immobilising toxic metals in fine granular contaminated soils (from Industrial Zones in South Korea). *International Journal of Environmental Research and Public Health* **18** (5), 2530–2543.

Ueng, Y., Wang, Y., Tsao, C., Chang, Y., Tung, S. & Hsu, J. 2020 Monitoring and assessment of oyster and barnacle larvae settlement in an oyster farm in western Taiwan. *Natural Resources* **11** (3), 112–126.

Vaschenko, M., Hsieh, H.-L. & Radashevsky, V. 2013 Gonadal state of the oyster *Crassostrea Angulata* cultivated in Taiwan. *Journal of Shellfish Research* **32**, 471–482.

Watanabe, T., Fujimoto, R., Sawai, J., Kikuchi, M., Yahata, S. & Satoh, S. 2014 Antibacterial characteristics of heated scallop-shell nano-particles. *Biocontrol Science* **19**, 93–97.

Wu, B., Li, J., Sheng, M., Peng, H., Peng, D. & Xu, H. 2022 The application of biochar and oyster shell reduced cadmium uptake by crops and modified soil fertility and enzyme activities in contaminated soil. *Soil* **8** (1), 409–419.

Xu, X., Liu, X., Oh, M. & Park, J. 2019 Oyster shell as a low-cost adsorbent for removing heavy metal ions from wastewater. *Polish Journal of Environmental Studies* **28** (4), 2949–2959.

Xu, Z., Valeo, C., Chu, A. & Zhao, Y. 2021 The efficacy of whole oyster shells for removing copper, zinc, chromium, and cadmium heavy metal ions from stormwater. *Sustainability* **13** (8), 4184–4206.

Yasue, S., Sawai, J. & Kikuchi, M. 2011 Sporicidal activity of heated dolomite powder against *Bacillus subtilis* spore. *Transactions of the Materials Research Society of Japan* **36**, 607–610.

Yasue, S., Sawai, J., Kikuchi, M., Nakakuki, T., Sano, K. & Kikuchi, T. 2014 Sporicidal characteristics of heated dolomite powder against *Bacillus subtilis* spores. *Biocontrol Science* **19** (3), 113–119.

Younis, S. A., El-Azab, W. I., El-Gendy, N. S., Aziz, S. Q., Moustafa, Y. M., Aziz, H. A. & Amr, S. S. A. 2014 Application of response surface methodology to enhance phenol removal from refinery wastewater by microwave process. *International Journal of Microwave Science and Technology* **2014**, 639457.

Zheng, X., Zou, M., Zhang, B., Lai, W., Zeng, X., Chen, S., Wang, M., Yi, X., Tao, X. & Lu, G. 2022 Remediation of Cd-, Pb-, Cu-, and Zn-contaminated soil using cow bone meal and oyster shell meal. *Ecotoxicology and Environmental Safety* **229**, 113073–113082.

Zhu, Y., Li, Q., Yu, H. & Kong, L. 2018 Biochemical composition and nutritional value of different shell color strains of Pacific oyster *Crassostrea gigas*. *Journal of Ocean University of China* **17** (4), 897–904.

First received 15 October 2022; accepted in revised form 3 February 2023. Available online 16 February 2023